Additive Manufacturing and Vulcanization of Carbon Black Filled Natural Rubber Based Components

Sebastian Leineweber[a, *], Lion Sundermann[b, *],
Lars Bindszus[a], Ludger Overmeyer[a], Benjamin Klie[b], Heike Wittek[b], Ulrich Giese[b]

[a] Institut für Transport- und Automatisierungstechnik
[b] Deutsches Institut für Kautschuktechnologie e.V.

[*] Corresponding authors: sebastian.leineweber@ita.uni-hannover.de,
Lion.Sundermann@DIKautschuk.de

ABSTRACT

Additive manufacturing of thermoplastics or metals is a well approved sustainable process for obtaining rapidly precise and individual technical components. Except for crosslinked silicone rubber or thermoplastic elastomers, there is no way of additive manufacturing elastomers. Based on the development of the *Additive Manufacturing of Elastomers* (AME) – process, the material group of rubber based cured elastomers may get first access to the process field of 3D-printing. Printing and crosslinking of rubber is separated in two steps: At first printing is realized by extrusion of the rubber by using a twin screw extruder, working according to a derived *Fused-filament-fabrication* (FFF) principle. In the second step the component is vulcanized in a high pressure hot-air autoclave. Due to the plastic flow behavior of non-crosslinked rubber materials a thermoplastic shell is probably needed to keep the geometry and position of the additively manufactured rubber in shape. In this way one layer of thermoplastic and one layer of rubber are printed alternatingly until the component is finished. Afterwards the manufactured binary component is placed in an autoclave to obtain the elastomer after vulcanization under hot air and high pressure atmosphere. Afterwards the thermoplastic shell gets removed from the elastomer and subsequently can be recycled. High viscosity of rubber during processing compared to conventional thermoplastics and an instable shape after extrusion is challenging in the development of the AME. This contribution will show a modified 3D-printer, explain the printing process from the designed component, via shell generation, to the vulcanized component and show first printed components.

INTRODUCTION

Additive manufacturing of thermoplastics or metals has become state of the art and is used in a wide range of areas, such as automotive engineering, aerospace and the manufacturing of medical products[1]. In contrast, the development of processes for the additive manufacturing of elastomers is still in its beginnings. Up to now, processes of additive manufacturing of elastomers have been based either on the processing of thermoplastic elastomers[2] or cross-linked silicone rubbers[3] such as nanosilica composite elastomers[4] or poly(2-methoxyethylacrylate)-silica composite elastomers[5][6]. However, the additive manufacturing of rubber-based elastomers in particular has posed major challenges to science to date. In one project, ground tire rubber was printed as a filler in a polymer matrix[7]. Otherwise, in parallel with the work carried out here (as far as the authors are aware), only the group of *Drossel et al.* is working in the field of extrusion based additive manufacturing of unvulcanized rubber-based elastomers[8]. In their research activity the utilized processing method differs fundamentally to the AME process and the process is limited to NBR based rubber compounds with a certain viscosity range at the moment[9].

Rubber based carbon black-filled elastomer materials in general offer a wide range of possible applications in the industry. Rubber is used in particular for seals[10], dampers[11] and tires[12]. In comparison to natural or other synthetic rubber, silicone rubber shows especially a highly temperature dependent chemical resistance and mechanical behavior, which has a negative impact on an alternative use of these materials instead of conventional rubber[13]. Additive manufacturing is used for production of prototypes[14] as well as for manufacturing of spare parts[15]. Especially the production of spare parts can be a sustainable aspect[16][17] for the rubber industry. Rubber ages during storage[18] so that stored rubber components are no longer usable after a few years due to their embrittlement. With just-in-time production, this waste of resources can be avoided[19]. Ageing behavior of rubber appears to be particularly disadvantageous if plant and plant-specific spare parts production are discontinued and stocks of rubber-based spare parts are no longer usable after a few years. As a consequence, otherwise functioning plants have to be shut down. This behavior can be countered by the sustainable use of additive manufactured spare parts, which prove to be economically and particularly ecologically profitable for companies and society as a whole[16][17].

These facts make clear that there must be a scientific interest in creating a process for additive manufacturing of rubber based carbon black filled elastomers. In contrast to conventional thermoplastics, high viscosity of rubber[13] and the plastic flow behavior[20] of non-vulcanized rubber pose a major challenge for additive manufacturing of carbon black filled rubber elastomers. Processing of a highly loaded polymer is necessary, to reduce the

extrudate distortion and die swell after passing the nozzle of the extruder. However, a high carbon black[13] loading but also a small particle size and high structure of the used carbon black increase the viscosity[21], which requires sufficient torque of the extruder, so that conventional thermoplastic extruder from the 3D-printing field are not suitable.

This work is based on the principle of the *Additive Manufacturing of Elastomers (AME)* - process developed by Wittek et al[22]. In this process, a thermoplastic, which acts as a shell material, and rubber are printed in layers in serial printing. Thus, in each layer the printed rubber is protected from flowing by a thermoplastic shell[22]. The process is based on *Fused Filament Fabrication (FFF)* - a method used for additive manufacturing of thermoplastics[23] [24]. The 3D-printer used is a FDM printer that has been extended by a small twin-screw extruder to deposit unvulcanized rubber in strands and layers on a printing table. Once the components have been printed, they must be vulcanized in their shells in a high pressure hot-air autoclave[22]. After vulcanization, the elastomer component is dimensionally stable[13] and the shell can be removed. The setup of the 3D-printer was shown in detail in a previous publication. Initial extrusion tests have also been carried out to determine the material throughput of the extruder[25].

At the beginning of this paper the output equipment and the materials used for printing are described. Subsequently, the printer developed for the AME-process is presented. Following, the process from the generation of a CAD file to the finished vulcanized component is briefly described using a process chain. However, the core of this work is an algorithm for generating a printable G-Code for the AME-process and a materials science evaluation of the process. First print results are displayed subsequently.

Preliminary tests have shown that a shell is not necessary for every component. The tensile specimens highlighted in this paper are stamped out from additive manufactured rubber plates, which were therefore printed without shell, and are then compared to specimen which were stamped out from a conventionally produced pressed rubber plate. In particular, the adhesive behavior of printed rubber strands among each other is evaluated without having to take complex geometries into account. Afterwards, the influence of a shell is shown by printed cuboids. Finally, a conclusion of the results is given.

EXPERIMENTAL

EXTRUDER SPECIFICATIONS

The rubber extruder is a co-rotating 9 mm twin screw extruder with a conveying screw design without any kneading elements from *Three-Tec GmbH* providing a maximum torque of

13 Nm. The pitch of the screws is 9 and the relation L/D is 20. Different rotational speeds can be adjusted from 0-200 rpm. Temperature can be controlled in three zones separately up to 200°C.

ADDITIVE MANUFACTURING UNIT FOR THERMOPLASTICS

The basic 3D-printer is a former CNC milling machine, converted to a FFF-Printer (Modell: *M3-3D* from *BZT Maschinenbau GmbH*). It has two high-temperature print heads for thermoplastic material that can be heated up to 400°C. The size of the printing area is 500 mm x 500 mm x 250 mm and the printing plate of this 3D-printer model is stationary. Thus, a layer change is achieved by moving the print heads up by one unit of length. The repeatability in printing process is 0.03 mm. The printing bed is a carbon printing plate, which can be heated up to 120°C in a closed construction space. Consequently, construction space can be heated by the plate.

HIGH PRESSURE HOT-AIR AUTOCLAVE

A high pressure hot-air autoclave from *Zirbus technology GmbH* with the designation *HDA-H 65-10-180* is used for vulcanization of the rubber components. The autoclave has a pressure chamber volume of 62 liters. Vulcanization itself can be performed at a pressure of up to 9.5 bar and up to 185 °C, making this autoclave ideal for the vulcanization of rubber.

MATERIALS

The natural rubber based recipe used in this study is used for windshield wiper blades. The formula is based on a “SVR CV 50” natural rubber with a Mooney viscosity ML (1+4) at 100°C of 50 MU ± 5. “Corax N 550” with a STSA of 39 m^2/g and an OAN of 121 ml/100 g is used as semi effective filler. The carbon black content is 40 phr. Additional additives and a sulfur-accelerator based curing system complete the formula. Mooney viscosity of the rubber compound is determined to Mooney ML (1+4) at 100 °C by means of a Monsanto “MV 2000 E” viscometer to 97 MU. It was measured with the large rotor, at a preheating time of 1 min and a testing time of 4 min. The shells are printed with a water-soluble polyvinyl alcohol- (PVA-) filament, which is printed at a nozzle temperature of 220 °C.

RESULTS AND DISCUSSION

SETUP FOR THE AME-PROCESS

Since the rubber viscosity is too high, even when heated, direct printing via integrated print heads of the 3D-printer is not possible. Therefore, the 3D-printer has to be modified for the AME-process. For this purpose, a twin screw extruder is integrated into the existing 3D-printer. The extruder has a sufficiently high torque to extract and print rubber. The extruder is assembled directly on the traversing unit of the 3D-printer as shown in Figure 1.

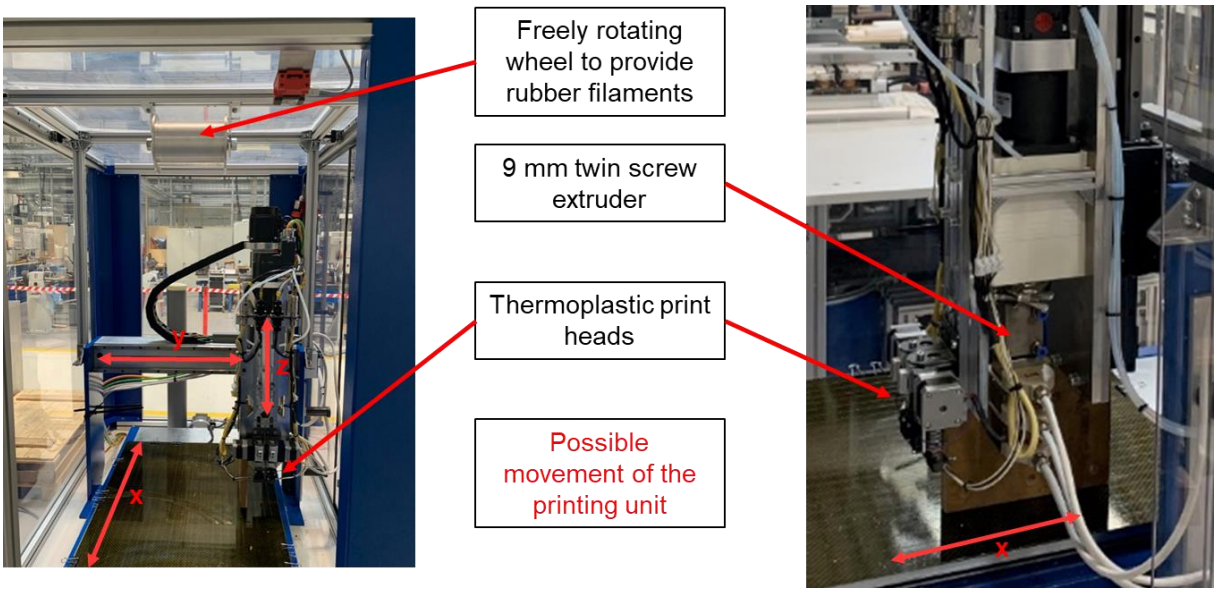

Figure 1. Setup of the new additive manufacturing plant for the AME-process

Since the extruder is approximately 12 kg heavier than the two original thermoplastic print heads of the 3D-printer, it was assembled as close as possible to the balance point of the traversing unit, minimizing the tilting moment. Thus, preventing vibrations during printing process, which might negatively affect printing resolution. The extruder is directly connected to the movement of the 3D-printer and only the feeding of rubber has to be controlled separately. The original print heads were assembled in front of the extruder. The control unit of the 3D-printer allows the selection of a print head for thermoplastic material or the extruder for rubber. However, the controller does not directly give the order for printing to the extruder. It sends the signal to the extruder's additionally post-implemented control unit which activates the extruder. An additional touch panel on the control unit of the extruder enables controlling of the feed rate, by adjusting the rotational speed of the screws. In general, speed values are fixed before the printing process starts, so that the control unit of the extruder only receives an order to start or to stop printing.

To ensure a continuous material feeding of the extruder, a freely rotating wheel is installed above the extrusion unit which is able to follow the movement of the 3D-printing unit in x-direction. The roller is wrapped with rubber filament before printing. During the process of printing, the material is fed by the extruder and continuously processed. Only a continuous material feed ensures a continuous material flow, which is required for a constant printing speed and a printed layer with a constant volume and a stable geometry.

THE PROCESS CHAIN

In order to manufacture rubber components by additive manufacturing, the steps shown in Figure 2 must be carried out. First of all, a component must be designed using Computer Aided Design (CAD) software and then converted into the STL-format, which has become established in additive manufacturing. Then, with help of the software *Autodesk Netfabb Premium 2019*, a shell with a freely selectable thickness is automatically generated and also converted into the STL-format. The shell is used to keep the non-vulcanized rubber in shape during the 3D-printing process and before vulcanization. Alternatively, the required shell can also be designed manually.

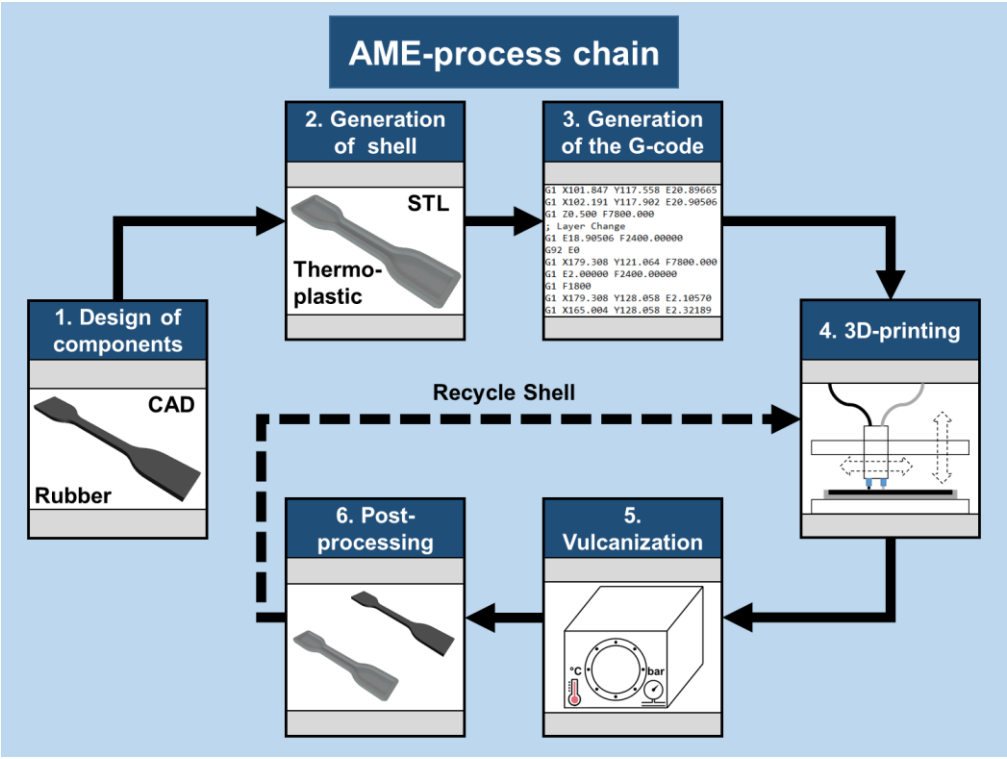

Figure 2. Process chain of the AME-process

The freeware *Slic3r* is used to generate a G-Code. However, the software has two significant disadvantages for the AME-process. On the one hand, the software only uses a travel optimized strategy, so-called “ABBA-strategy” for generating a G-Code. This means that first a shell (A) is printed in one layer, then a core (B) in the same layer and in the next layer first a core (B) is printed followed by a shell (A) and so on. This printing behavior would result in possibly non-geometrically stable rubber layers, which are printed before the thermoplastic in every second printing step, making this strategy unsuitable for the AME-process. On the other hand, the software does not provide a setting for different resolutions. This means different layer thicknesses for the rubber extruder and the thermoplastic print head are not possible, although the thermoplastics could be printed with a much thinner layer height than the rubber. This should be preferably done, to minimize imprints of layer structures covered by the rubber surface, which occur due to the flowability of the rubber material until vulcanization has stabilized its geometry.

Therefore, a G-Code for the shell and the component should be generated separately. It is important to ensure that the offset between the thermoplastic print head and the rubber extruder is also entered into the slicing software so that the component is located inside the shell during printing. Furthermore, the resolution of the thermoplastic shell must be a fraction of the resolution of the rubber component so that layers are always completed after the rubber has been printed. For a rubber resolution of 0.9 mm, either a resolution of 0.3 mm or 0.15 mm of a shell would be possible. An even finer resolution is also conceivable, if the 3D-printer used technically permits this.

In order to merge the two generated G-Codes back into one G-Code a software with a sorting algorithm was developed, which is described in the next subchapter and enables the generation of a G-Code that corresponds to a printing strategy of the type xA→B→xA→B. Whereby x represents number of layers of thermoplastic material to be printed. The print speed of 20 mm/s is set in *Slic3r*. Preliminary tests have shown that printing speed of 20 mm/s is suitable for the manufacturing of rubber.

After the G-Code has been modified by the independently developed software for the AME-process, 3D-printing can begin. The selected rubber is printed at a temperature of 100 °C and the material of the shell is printed at a temperature of 220 °C. 3D-printing is followed by vulcanization in a high pressure hot-air autoclave. The selected parameters are described in more detail in the section on the analysis of the components. After vulcanization, components are released from their shells and, if necessary, cleaned of thermoplastic residues in post-processing.

MODIFICATION OF THE G-CODE

First of all, the information on layer thickness of a component and its shell and on thickness of the bottom of the shell in a graphical user interface (GUI) have to be entered. Then the G-Codes of the shell and component, which are generated in the freeware *Slic3r* are imported one after the other, pre-sorted and post-processed. Post-processing includes removal of individual G-Code commands that disturb the process and the identification of crossings without printing in the G-Code of the rubber component. Finally, the pre-sorted and post-processed G-Codes are merged into one common Code.

Figure 3 illustrates the composition of an exemplary G-code for the AME process with a printing strategy of the type xA→B→xA→B. Whereby always two layers of the shell and then one layer of the component are printed. In the following the generation by the sorting algorithm is described step by step.

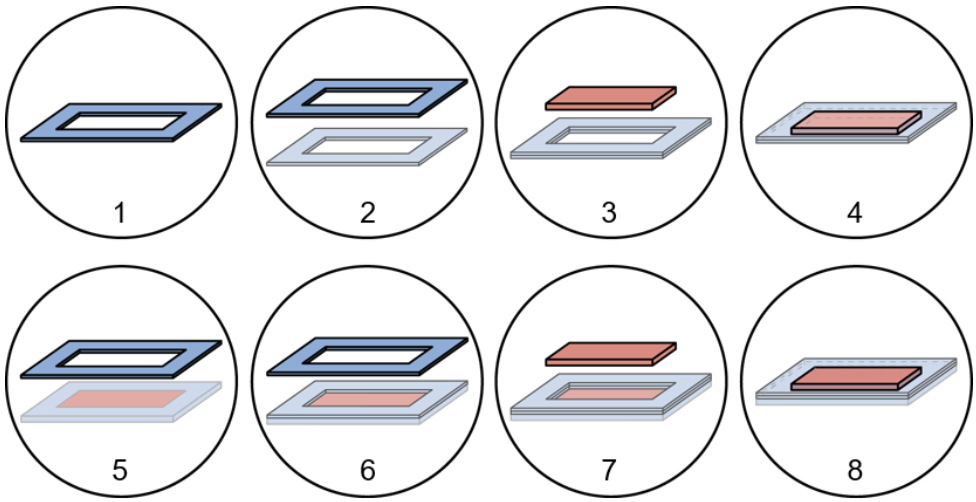

Figure 3. Exemplary illustration of a G-code for the AME-process

Pre-sorting of the component G-Code. – First, the entire G-Code of the component is imported line by line and searched for the end of the start sequence and the beginning of the end sequence. The general settings for 3D printing are stored in these two sections. Only lines within this area are relevant for sorting, since this area contains the traversing and extrusion commands for all layers. Finally, the lines of start and end sequence are inserted before and after the sorted area. The G-Code follows a scheme in which each layer is initiated by a layer change command, which is then followed by all traversing and extrusion commands of this layer. The algorithm takes advantage of this fact and divides the G-Code into two lists. In a first list, all travel and extrusion commands of a layer are grouped into

blocks, and in a second list all layer change commands are stored. Once the entire G-Code has been processed, both lists contain as many entries as there are layer changes.

Pre-sorting of the shell G-Code. – The procedure for pre-sorting the shell G-Code differs from that of the component G-Code, because the generation of the component G-Code is already done differently in *Slic3r.* To avoid the generation of support structures at overhangs inside the shell, the model of the component is positioned inside the shell and both geometries are sliced with a layer thickness of the shell as a multi-material print. The resulting G-Code shows areas of the shell as well as areas of inner component, which are identified by the tool change commands T0 and T1. Since the G-Code of the component with a higher layer thickness has already been generated and presorted, only the part of the shell, which gets initiated by the T0 command, is required from this G-Code.
Presorting of the shell G-Code is a two-step process. At first the G-Code is searched line by line for a layer change and the tool change commands T0 and T1. All areas of the shell belonging to extruder T0 are stored inside a list together with the layer change commands. In the second step, the G-code is then presorted according to an analogous procedure as for the G-code of the component.

Detect crossings without printing in the component G-Code. – When an extruder is repositioned within a layer, it is done, without printing, by crossings. A crossing consists of a move command without an extrusion command. In contrast to the thermoplastic extruder, the rubber extruder cannot differentiate between crossings and normal extrusion commands. To ensure that no rubber is extruded during crossings, the rubber extruder must be switched off before a crossing starts and switched on again after a crossing. The detection of crossings is done by the speed information F7800 in the move command of the G-Code. If this is detected, the commands for switching on and off the extruder are inserted before and after that line.

Merging to one G-Code. – Once the G-Codes of the component and shell have been sorted and post-processed, they are merged into one common G-Code in a two-stage process. In the first step the layers are sorted that belong to the bottom of the shell and therefore only to the thermoplastic extruder. A shell bottom is present if the input thickness of the bottom of the shell is greater than 0. However, if the thickness of the bottom is 0, then there is only a vertical shell and no bottom, so that the second step of sorting can be started immediately.
The second step sorts the area in which the layers of the shell and component alternate. In this case, the shell is printed first in each layer, and if the G-codes of the component and shell have different layer thicknesses, it is necessary to print as many layers of the shell until

they have the same thickness as one layer of the component. Following this procedure, the layers of the shell and the layers of the component are printed alternately until all blocks of the component have been sorted. The required tool change command is inserted before each block. Finally, the lines belonging to the start and end sequence are inserted before and after the sorted area. In the end, all lines are exported as a common G-code.

ANALYSIS OF THE PRINTED COMPONENTS

Tests were carried out in order to find the optimal vulcanization time. At 150 °C the vulcanization time t_{90} was 7 min 20 s. This duration was used for the manufacturing of a reference sample in a conventional heat press process. However, it has to be considered that heat transfer inside the hot air autoclave is significantly lower than inside the heating press, so that the vulcanization time has to be increased. To manufacture the reference samples, S2-tensile specimens were stamped out from a rubber plate of 2 mm thickness, manufactured in a heating press at a temperature of 80 °C and a pressure of 280 bar for several minutes. At this temperature vulcanization is not initiated yet. The stamped out test specimens were vulcanized in the autoclave with 5 different time periods at 150 °C and 7 bar. In Table I the results of the tensile test for the vulcanized specimen are compared with the unvulcanized specimen and the vulcanized reference sample.

Table I. Varied vulcanization time of NR based rubber mixture at 150 °C

Vulcanization Time, min	Tensile strength, MPa	Elongation at break, %	Stress at 100 % strain, MPa	Stress at 200 % strain, MPa	Stress at 300 % strain, MPa
0 min	0.8±0.1	205±60	0.5±0.1	0.7	-
7 min	23.7±4.4	568±7	1.5±0.4	3.9±0.9	7.2±1.5
15 min	22.8±2.1	513±40	2.3±0.2	5.6±0.4	9.7±0.5
30 min	12.0±1.4	325±40	2.7±0.1	6.3±0.2	10.4±0.2
45 min	7.1±1.7	220±40	2.6±0.1	6.2±0.2	-
60 min	6.5±0.4	209±13	2.7±0.1	6.0±0.2	-
Reference sample	21.9±4.1	462±60	2.7±0.1	6.3±0.1	10.8±0.1

Comparing the value of the unvulcanized specimen with the values of the vulcanized specimens, it is obvious that the curing process in the autoclave was successful. The reference sample provides a tensile strength of 21.9 MPa and an elongation at break of 462 %. Here, the sample with 7 and 15 min vulcanization time respectively show the most similar material behavior with tensile strength of 23.7 MPa and 568 % elongation at break and 22.8 MPa and 513 % respectively, which are in range of error. The latter show a stronger increase of stress by increasing stress, which might be observed due to a more homogeneous curing process. By further increasing the time inside the autoclave, the values of the maximum tensile strength decrease significantly due to reversion of the natural rubber, as well as maximum elongation at break. Because of the increasing stress values at 100 % strain with longer vulcanization time, it can be assumed that an embrittlement of the material occurs. For that reason, 15 min was set as vulcanization time in the autoclave for further tests.

All 3D-printing tests with rubber were carried out with a nozzle diameter of 1 mm, resulting in a strand diameter of 1.3 mm due to swelling[26]. A smaller nozzle diameter and thus a higher print resolution was not possible with the selected rubber compound and the extruder used since the extruder reached its torque limit. A decrease in viscosity of the used rubber mixture to enable extrusion through a smaller nozzle is limited by following aspects, and can be content of further studies: Firstly, the reduction of carbon black content as a filler would lower the filler filler network stability and cause a stronger distortion of the extrudate[21], that the dimensional stability cannot be ensured, despite the presence of a thermoplastic shell. Secondly, low viscous feeding stripes tear off in the feeding zone due to insufficient screw design influencing the intake bahavior and resulting in an instable volume flow.

For first printing tests the nozzle distance to the table was set to 0.9 mm, which is slightly smaller than the stripe diameter of about 1.3 mm, squeezing the rubber strand onto the printing plate. This causes the stripes to be wider. The temperature of the extruder was set to 100 °C and the rotational speed was set to 40 rpm which corresponds to a printing velocity of 1.98 mm/s. Before printing first geometrically complex parts, the influence of the distance between two printed stripes on the mechanical properties had to be investigated. Therefore, additive manufactured rubber plates consisting of two additively manufactured rubber layers with different stripe distances from 1.2 to 1.6 mm were manufactured in a parallel printing pattern to observe the influence of adhesion of neighboring stripes. A filling density of 100 % is adjusted in the slicing software.

The tensile test specimens were stamped out of the respective plate, vulcanized and tested at a 90 ° angle to the printing direction, which is illustrated in Figure 4.

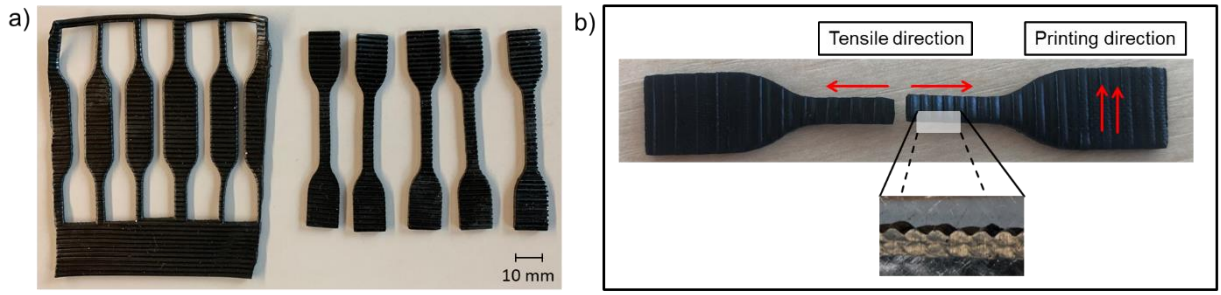

Figure 4. S2 tensile specimens a) Stamped out specimen before vulcanization b) scheme of a single S2 specimen after a tensile test (test direction perpendicular to print direction, parallel printing pattern)

The values of the tensile tests are shown in Table II. The highest tensile strength shows the sample with a stripe distance of 1.2 mm, as well as a maximum elongation at break (495 %). During the printing process, the stripes in each single layer have the greatest overlap among each other, which leads to a higher stability of the additive manufactured part. However, the deviation of the standard thickness is very high (+30 %). The best dimensional accuracy provides the sample of 1.4 mm stripe distance showing reasonable values of tensile strength of 13.9 MPa and 421 % elongation at break. If the stripe distance is further increased, the mechanical properties decrease.

Table II. Tensile tests of S2 specimens to determine the optimal stripe distance

Test specimen	Tensile strength, MPa	Elongation at break, %	Stress at 100 % strain, MPa	Stress at 200 % strain, MPa	Stress at 300 % strain, MPa	Deviation from standard thickness, %
Reference sample	21.9±4.1	462±60	2.7±0.1	6.3±0.1	10.8±0.1	0
1.2 mm nozzle distance	16.5±1.2	495±19	1.6±0.1	4.0±0.2	7.4±0.3	approx. +30
1.4 mm nozzle distance	13.9±1.1	421±20	1.8±0.1	4.5±0.2	8.1±0.3	approx. +0.5
1.6 mm nozzle distance	12.7±0.5	406±30	1.7±0.2	4.3±0.3	7.8±0.5	approx. -15

To neglect adhesion of the stripes among each other, samples were manufactured with 1.4 mm stripe distance and were tested for their tensile properties in printing direction. Also, further S2-specimens were manufactured, using a crossed printing strategy, which means that the layers were printed in an alternating angle of 90°, improving the isotropy of the

sample. In this case two different tests were done. In one test the upper layer is teared in printing direction and in the other test the lower layer teared respectively. The results of the tensile tests are shown in Table III.

Table III. Tensile tests of S2 specimens with different printing patterns

Printing strategy of the specimen	Tensile strength, MPa	Elongation at break, %	Deviation from standard thickness, %
Reference sample	21.9±4.1	462±60	-
Parallel; test direction is printing direction	24.8±2.4	580±50	approx. +10
Crossed; printing direction of upper layer in test direction	13.6±0.5	470±12	approx. +25
Crossed; printing direction of lower layer in test direction	14.3±0.8	453±20	approx. +30
Parallel; test direction is 90° to printing direction	13.9±1.1	421±20	approx. +0.5

From Table III it can be deduced, that the highest tensile strength and elongation at break (24.8 MPa, 580 %) is obtained, when the specimen is teared in the direction of printing. That is because the main contribution to the mechanical stability is provided by the material properties, rather than the quality of the adhesion between the stripes after additive manufacturing. Otherwise the crossed printing patterns reveal a better anisotropic behavior and show no significant difference between the order of the printed layers. However, the mechanical properties are lower compared to the specimen, that is printed parallelly and tested in printing direction. To investigate better the influence of the printing strategies, parts with more layers have to be manufactured to find out if hereby an improvement can be achieved. The tensile strength of the crossed test specimens is reduced by about 44 % compared to the non-crossed sample which is teared in printing direction.

In order to print more complex and voluminous rubber parts, first printing tests of rubber cuboids with a dimension of 50 mm x 50 mm x 9.9 mm were carried out. The initial adhesion especially of the rubber part to the printing bed is challenging, so that double-sided adhesive tape had to be attached to the printing bed for increased adhesion. The shell is built up using a concentric printing strategy, whereas the rubber part is printed in a crossed printing pattern from one layer to another, except for three concentrically surrounding layers.

In Figure 5 the effect of the thermoplastic shell on the additive manufactured rubber part is illustrated. Both parts, with and without a thermoplastic shell, could be printed successfully. It is obvious that in this case for geometrically simple parts a shell structure is not required.

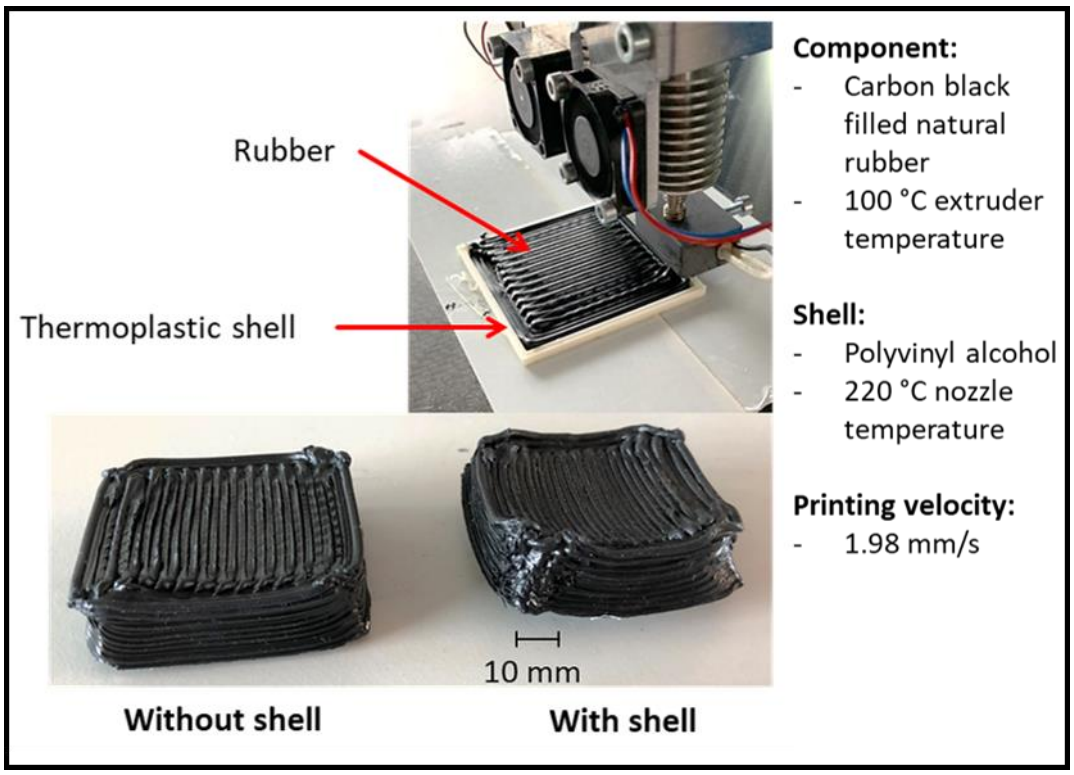

Figure 5. Comparison of an additively manufactured rubber part with and without thermoplastic shell

Shells gain in importance for components with bridges or overhangs. Additionally, an accelerated curing system could improve dimensional stability due to scorching either immediately after the printing process or in the autoclave in a second step. However, scorching inside the extruder has to be prevented. Moreover, scorching directly after passing the nozzle might lower the adhesion between the printed layers due to reduced flowability. Furthermore, the increased printing temperature of 220 °C for the HT-PVA leads to a significant heat conduction into the rubber part leading to an enhanced heat distortion. The use of a heating system for the chamber volume of the 3D printer could prevent a cool down of the already printed rubber layers. Thus, the temperature difference of rubber and thermoplastic is decreased, which might reduce the heat distortion and increase the dimensional stability as well. However, this may lower the adhesion of the first printing layer on the bed by melting the glue of the double-sided adhesive tape.

Another approach would be the use of a thermoplastic material with a significantly lower melting point allowing lower processing temperatures during additive manufacturing. However, it is important to note that the dimensional stability of this thermoplastic material

may no longer be sufficient for the additively manufactured rubber part at the vulcanization temperatures used in the autoclave. Due to the early melting of the thermoplastic shell, the rubber compound, which is still flowable at the beginning of the vulcanization process, could lose the desired geometric shape.

CONCLUSION

This paper deals with the development, construction and testing of a 3D-printing system for additive manufacturing of rubber parts. It has been demonstrated that the main principle of the AME-process for additive manufacturing of carbon black filled rubber parts is a promising technology. The developed system is based on a 3D-printer for the additive manufacturing of thermoplastic components from *BZT Maschinenbau GmbH*. In addition, a 9 mm twin-screw extruder from *Three-Tec GmbH* is used to allow rubber printing. The rubber strips are fed continuously. The 3D-printer enables the additive production of rubber compounds and thermoplastics in a serial process by alternately printing thin layers of thermoplastics for the shell and rubber for the component.

The process chain of the AME-process was described as a six-stage process. First a desired rubber part has to be designed and converted into STL format. Second a thermoplastic shell is computer aided automatically generated. Afterwards, the printable G-Codes of the part and its shell are generated separately. The G-Codes are merged by a program in a way that each printed layer of thermoplastic is followed by a layer of rubber. With a higher resolution of the thermoplastic, several layers of thermoplastic are printed first before a layer of rubber follows. The program generates blocks for both G-Codes with a single printing layer depending on the height coordinate z before merging them to a printing strategy of the type xA→B→xA→B. The following vulcanization of the rubber component in its thermoplastic shell is then performed inside an external autoclave process. Finally, the rubber part is removed from its shell and, if necessary, post-processing is carried out.

The NR based rubber plates were printed with an extruder temperature of 100 °C and a distance of 0.9 mm between the nozzle and the printing bed and subsequently vulcanized in the autoclave at 150 °C and 7 bar for 15 minutes. By using the stamped out tensile specimens from the rubber plates it was determined that a strand spacing of 1.4 mm within each printed layer is recommended. Ultimately, with an ideal print sample, the additively produced samples achieve a comparable tensile strength to conventionally produced samples. It has been demonstrated that shells are not necessary for simple components because, at least for the rubber compound used, the viscosity is high enough to prevent flow behavior after additively manufacturing. Moreover, the use of shells is difficult, as there is an additional heat input into the rubber components, which can lead to heat distortion.

Therefore, shells should only be used for components with bridges or overhangs or if the rubber compounds used feature a lower viscosity and an increased flow behavior immediately after additive manufacturing of the strand.

ACKNOWLEDGEMENT

We owe thanks to the German Federation of Industrial Research Associations *Otto von Guericke e.V*. (AiF) and its member association *Deutsche Kautschuk Gesellschaft e.V.* (DKG) for financial support provided for work on IGF project 20527 N, funded by the *Federal Ministry for Economic Affairs and Energy* (BMWi). We also like to thank *Three-Tec GmbH* for technical support to implement the twin screw extruder in an additive manufacturing process.

REFERENCES

[1] T. T. Wohlers, *Wohlers report 2012*. *Additive manufacturing and 3D printing state of the industry: annual worldwide progress report*, Wohlers Associates, Fort Collins, Col., **2012**.

[2] K. Elkins, H. Nordby, C. Janak, Gray, IV, W. Robert, J. Helge Bohn, D. G. Baird in *1997 International Solid Freeform Fabrication Symposium*, **1997**.

[3] J. Stieghorst, D. Majaura, H. Wevering, T. Doll, *ACS applied materials & interfaces* **2016**, *8*, 8239.

[4] L.-Y. Zhou, Q. Gao, J.-Z. Fu, Q.-Y. Chen, J.-P. Zhu, Y. Sun, Y. He, *ACS applied materials & interfaces* **2019**, *11*, 23573.

[5] F. Asai, T. Seki, A. Sugawara-Narutaki, K. Sato, J. Odent, O. Coulembier, J.-M. Raquez, Y. Takeoka, *ACS applied materials & interfaces* **2020**, *12*, 46621.

[6] T. J. Hinton, A. Hudson, K. Pusch, A. Lee, A. W. Feinberg, *ACS biomaterials science & engineering* **2016**, *2*, 1781.

[7] F. Alkadi, J. Lee, J.-S. Yeo, S.-H. Hwang, J.-W. Choi, *Int. J. of Precis. Eng. and Manuf.-Green Tech.* **2019**, *6*, 211.

[8] W.-G. Drossel, J. Ihlemann, R. Landgraf, E. Oelsch, M. Schmidt, *Polymers* **2020**, *12*.

[9] W.-G. Drossel, J. Ihlemann, R. Landgraf, E. Oelsch, M. Schmidt, *Materials (Basel, Switzerland)* **2021**, *14*.

[10] T. R. Vijayaram, *Int. J. Design Manufact. Technol* **2009**, *3*, 25.

[11] A. Nakamura, A. Kasuga, H. Arai, *Construction and Building Materials* **1998**, *12*, 115.

[12] D. Nelson, *J. Eco. History* **1987**, *47*, 329.

[13] F. Röthemeyer, F. Sommer, *Kautschuk-Technologie*. *Werkstoffe - Verarbeitung - Produkte*, Hanser, München, **2013**.

[14] J.-P. Kruth, M. C. Leu, T. Nakagawa, *CIRP Annals* **1998**, *47*, 525.

[15] S. H. Khajavi, J. Partanen, J. Holmström, *Computers in Industry* **2014**, *65*, 50.

[16] S. Ford, M. Despeisse, *Journal of Cleaner Production* **2016**, *137*, 1573.

[17] W. W. Wits, J. R. R. García, J. M. J. Becker, *Procedia CIRP* **2016**, *40*, 693.

[18] K. Reincke, B. Langer, S. Döhler, U. Heuert, W. Greilmann, *KGK Kautschuk Gummi Kunststoffe* **2014**, *2014*, 60.

[19] S. Phogat, A. K. Gupta, *J of Qual in Maintenance Eng* **2019**, *25*, 25.

[20] C. H. Schroeder, *Rubber Chemistry and Technology* **1952**, *25*, 651.

[21] J. L. White, J. W. Crowder, *J. Appl. Polym. Sci.* **1974**, *18*, 1013.

[22] H. Wittek, B. Klie, U. Giese, S. Kleinert, L. Bindszus, L. Overmeyer, *KGK-KAUTSCHUK GUMMI KUNSTSTOFFE* **2019**, *72*, 53.

[23] S. S. Crump, *Apparatus and method for creating three-dimensional objects*, **1992**, Google Patents.

[24] S. S. Crump, J. W. Comb, W. R. Priedeman Jr, R. L. Zinniel, *Process of support removal for fused deposition modeling*, **1996**, Google Patents.
[25] L. Sundermann, S. Leineweber, B. Klie, U. Giese, L. Overmeyer, *KGK-KAUTSCHUK GUMMI KUNSTSTOFFE* **2020**, *73*, 30.
[26] C. Price, *Proc. R. Soc. Lond. A* **1976**, *351*, 331.